International Journal on Emerging Technologies **11**(1): 263-269(2020)

ISSN No. (Print): 0975-8364
ISSN No. (Online): 2249-3255

Assessment of Land Use and Land Cover Dynamics in Shingla River Basin Using Multi Temporal Satellite Imageries

Abdullah Salim Khan[1] and Anisa Basheer Khan[2]
[1]Research Scholar, Department of Ecology and Environmental Sciences, Pondicherry University, Kalapet, Puducherry 605014, India.
[2]Former Professor, Department of Ecology and Environmental Sciences, Pondicherry University, Kalapet, Puducherry 605014, India.

(Corresponding author: Anisa Basheer Khan)
(Received 14 October 2019, Revised 16 December 2019, Accepted 23 December 2019)
(Published by Research Trend, Website: www.researchtrend.net)

ABSTRACT: Shingla River Basin (SRB) with a catchment area of about 790 sq. km, spread along the southern Assam's Karimganj district and part of Mamit district in Mizoram has a large forest cover and diverse physiographic features. Large scale reduction in forest cover and landscape changes pose severe threat to the biodiversity of the basin. Accurate estimation of long-term changes occurring in large river basin is a big challenge. The difficulties involved in accurate quantification of land use and land cover changes are: range of data, procedural and analytical complications associated with diverse phenomena, space–time patterns and social and biophysical processes. In the present study, multi-temporal satellite imageries were used to assess Land Use and Land Cover (LULC) changes in Shingla river basin from 1975 to 2018. Satellite imageries viz., Lands at 1 MSS (1975), IRS-Resources at 1 LISS III (2008) and Sentinel 2-A MSI (2018) were used to assess the LULC changes in Shingla river basin. Maximum likelihood classifier (MLC), a supervised classification method in QGIS SCP (Semi-Automatic Classification Plugin) was used to generate LULC maps of Shingla river basin for the year 1975, 2008 and 2018. Four LULC classes were selected for assessing LULC changes. Results reveal that vegetation cover in SRB witnessed a steady decrease from 72.45% in 1975 to 58.91% in 2018. Built-up areas increased linearly from 3.71% in 1975 to 12.24% in 2018. However, temporal changes in croplands and water bodies were not linear. Croplands increased from 17.46% (1975) to 22.49% (2008) and then decreased to 19.18% (2018). Similarly, water bodies increased from 6.37% (1975) to 11.06% (2008) and then decreased to 9.65% (2018). Using Kappa statistics, overall accuracy for the result was found to be 93.77% with a Kappa co-efficient value as 0.86. The findings of the present study are useful for planners and decision makers in sustainable natural resource management and degradation mitigation strategies.

Keywords: Land Use and Land Cover, QGIS-SCP, Satellite imageries, Supervised classification, Shingla river basin (SRB).

I. INTRODUCTION

Globally the rate of land use and land cover (LULC) change has accelerated, more prominently in regions with high population growth [1]. Numerous factors associated with LULC dynamics are related to agricultural and environmental change [2, 3]. Changes in land use and land cover are impacted mainly by a complex interaction of social and ecological factors [4]. Natural resource management, climate change and rural and urban landscape planning are important issues which require a comprehensive understanding of land use and land cover change [5]. At basin level LULC dynamics alters most of the hydrological processes like evapotranspiration (EV), ground water recharge and overland flow [6]. Impact of LULC change on river basin hydrology is of great concern [7] as it can lead to water scarcity, flood risk and soil erosion [8]. Hydrological responses of a river system and climate variables are greatly influenced by the phenomena associated with land use and land cover change [9-10]. Both water quality and supply are affected by large scale changes in land use and land cover [11].

Proper assessment, precise and timely monitoring of LULC change is essential for effective natural resource management and climate change mitigation [12-13].
Shingla river basin which covers parts of the districts of Karimganj and Mamit in north-east India's states of Assam and Mizoram respectively, has undergone considerable population growth over the last few decades. The increasing population in SRB has impacted change in landscape pattern causing large scale reduction in forest cover. Shingla watershed with its channel networks irrigates a large portion of the basin which meets the water demand of the region for cultivation as well as vegetation growth. Remote sensing and GIS technology minimize both time and effort to assess LULC changes especially for large areas. Though a number of studies to monitor LULC changes using commercial and proprietary remote sensing and GIS softwares are available, works on LULC dynamics using free and open source softwares are few and far between with an obstacle for those researchers with no access to these expensive research tools. The present work is an attempt to provide scope for research on LULC dynamics using free and open source softwares.

Quantum GIS- a free and open source GIS software with a plug in called Semi-automatic Classification Plugin (SCP) is used for remote sensing and GIS analysis. The objective is to quantify major land use and land cover classes in Shingla river basin and detect their changes over four decades (1975 to 2018) using multi-temporal satellite remote sensing data.

II. MATERIALS AND METHODS

A. Study area

The area under study is the Shingla river basin (SRB) drained by river Shingla and the adjoining streams. SRB is a sub-basin of another major river basin called Barak river basin which forms the Barak valley in southern Assam, India. Shingla river basin extends from the hills of Mamit district in Mizoram to the south-western plain of Karimganj district in Assam. Shingla river basin with a catchment area of 790 sq km and forms a radial drainage system with a number of small watersheds formed by streams along its course. Using vector data digitized in Google Earth Pro (Version 7.3.2) and QGIS (Version 3.8.2), the total catchment area, the length, and the direction of the Shingla river course were estimated. Shingla originates at an altitude of 365 meters above sea level in the hills of Mamit district in Mizoram which are the offshoots of the Jampui hills located in Tripura. The basin also includes an important wetland in the downstream called Son Beel wetland, the largest freshwater wetland in Assam [14].

The wetland, which is also a potential Ramsar site serves as an outlet for river Shingla [15]. River Shingla travels in the north-south direction from the source to the outlet, traversing a distance of about 80 km. Shingla bifurcates, beyond the wetland into two distributaries which are locally known as Kuchua and Kakra. The Kuchua courses 23 km along the north-south direction and joins river Kushiara at the frontiers of India and Bangladesh. River Kakra, on the other hand, moves along the north-western direction traversing a distance of about 93 km and connects to the Kushiara River in Bangladesh which finally falls in the Bay of Bengal.

B. Study area map

Shingla river basin is bounded within 24º47′54″ to 24º09′40″ north latitude and 92º24′5″ to 92º27′04″ east longitude. Fig. 1 illustrates Shingla river basin including Son Beel wetland and the outlets of the river along with elevations in meters above mean sea level (AMSL). Shingla catchment boundary is delineated using SRTM DEM (30-meter spatial resolution) in Quantum GIS [16] and SAGA (System for Automated Geoscientific Analyses) software.

On-screen digitization is one of the most convenient methods and accurate technique for tracing and locating map features using a reference map [16-17]. This method is used for tracing Shingla river course and Son Beel wetland boundary in QGIS and using Google earth Pro as a base map. In field GPS tracked shape files and field surveyed data are also used.

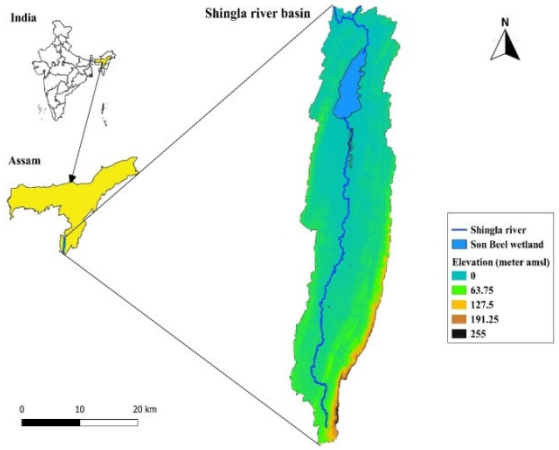

Fig. 1. Study area map depicting Shingla catchment and Son Beel wetland with elevation.

C. Soil in Shingla basin

The soil type in the upstream regions of Shingla river basin which lies in the hills of Mizoram, mostly belong to the soil order inceptisols [18]. Inceptisols are the prominent soils found in the mountainous regions which are characterized by high silt/clay ratio and are very susceptible to erosion [19]. On the other hand, soil in the downstream regions of Shingla river basin are fine loamy, mixed, hyperthermic which belong to the family of Endoquepts [20]. Soil map of Shingla river basin (Fig. 2) is created in QGIS based on the field collected soil sample analysed. It is observed that the soil in Shingla river basin is mostly older alluvium having a texture of clay loam. In some parts it is sandy loam in texture. The observed pH of the soil ranges from 4.5 to 6.0.

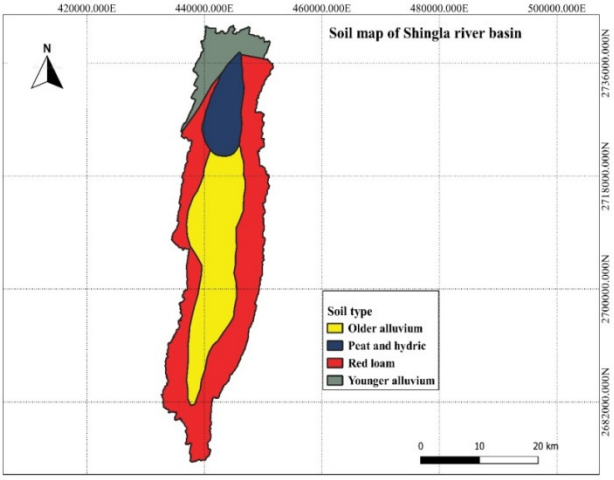

Fig. 2. Soil map of Shingla river basin generated in QGIS using field survey and NBSS Soil data.

D. Vegetation

The vegetation type in Shingla river basin varies from dense to open forest. In the upstream regions which fall in the hilly terrains of Mizoram, the basin has mostly dense forest but the downstream regions are dominated by open forest. Shingla river basin includes an ecologically significant forest zone called Shingla Reserve Forest which extends to Hailakandi district,

Mizoram, parts of Tripura [21] and this is a predominantly mixed evergreen and deciduous forest.

NDVI (Normalized Difference Vegetation Index) map showing the vegetation extent of Shingla river basin is created in QGIS using Sentinel 2 satellite data of the year 2018 (Fig. 3).

Calculation of NDVI [22] is based on the following equation:

$$NDVI = \frac{\rho_{nir} - \rho_{red}}{\rho_{nir} + \rho_{red}} \quad (1)$$

Where, ρ_{nir} represent reflectance at the Near Infra Red (NIR) wavelengths (0.7-1.1 µm) and ρ_{red} represent reflectance at the Red wavelengths (0.6-0.7 µm)

For Sentinel 2 satellite data, NIR is band 8 and Red is band 4. Hence, Eqn. (1) can be re-written as

$$NDVI = \frac{\rho_{band8} - \rho_{band4}}{\rho_{band8} + \rho_{band4}} \quad (2)$$

NDVI values range from –1 to +1 with higher values indicating dense vegetation and lower values representing sparse vegetation. In Shingla river basin NDVI values were found to vary from –0.461 to +0.862 with higher NDVI values observed in the upstream regions while the downstream regions showing lower NDVI values.

E. Satellite and ancillary data used

Remote sensing satellite data used includes Landsat-1 MSS (GLS), IRS LISS-III and Sentinel 2 for the period of 1975, 2008 and 2018 respectively, with details depicted in Table 1. Shingla river basin comprised of only one Landsat scene (path 146, row 43), eight IRS LISS III tiles and two Sentinel 2 tiles. WGS (World Geodetic System) 84 datum and Universal Transverse Mercator (UTM) projection is used in this study. Shingla river basin lies in the UTM zone 46N. Hence all the satellite images are projected to WGS 84/ UTM Zone 46 N.

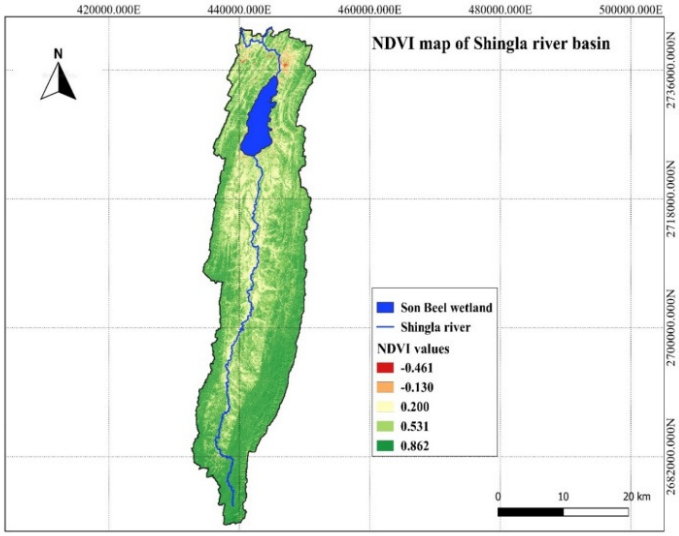

Fig. 3. Normalized Difference Vegetation Index (NDVI) map of Shingla river basin using Sentinel 2 image.

Table 1: Details of the satellite data used.

S.No.	Satellite Name	Sensor	Acquisition date	Path/Raw/Tile	Spatial resolution (meter)	Source
1.	Landsat 1	MSS	26-03-1975	146/43	60	USGS
2.	IRS Resourcesat 1	LISS III	19-11-2008	G46U05	23.5	NRSC, ISRO
3.	IRS Resourcesat 1	LISS III	19-11-2008	G46U06	23.5	NRSC, ISRO
4.	IRS Resourcesat 1	LISS III	19-11-2008	G46U07	23.5	NRSC, ISRO
5.	IRS Resourcesat 1	LISS III	19-11-2008	G46U08	23.5	NRSC, ISRO
6.	IRS Resourcesat 1	LISS III	19-11-2008	G46U09	23.5	NRSC, ISRO
7.	IRS Resourcesat 1	LISS III	19-11-2008	G46U10	23.5	NRSC, ISRO
8.	IRS Resourcesat 1	LISS III	19-11-2008	G46U11	23.5	NRSC, ISRO
9.	IRS Resourcesat 1	LISS III	24-11-2008	G46U12	23.5	NRSC, ISRO
10.	Sentinel 2 A	MSI	30-12-2018	T4QDM	10	ESA, Copernicus
11.	Sentinel 2 A	MSI	30-12-2018	T46RDN	10	ESA, Copernicus

QGIS version 3.8.2, a freely available open source GIS software is used for both remote sensing and GIS analysis. QGIS has an important plug-in called SCP (Semi-automatic Classification plug-in) which is used for satellite image processing, study area extraction and Land Cover Land Use Classification. Final map is also generated in QGIS map composer using raster data and digitized vector data. SAGA (System for Automated Geoscientific Analyses) is used for Shingla river catchment delineation using 30 meters SRTM DEM.

Pixel based maximum likelihood supervised classification method is used for LULC classification in Shingla river basin (Fig. 4).

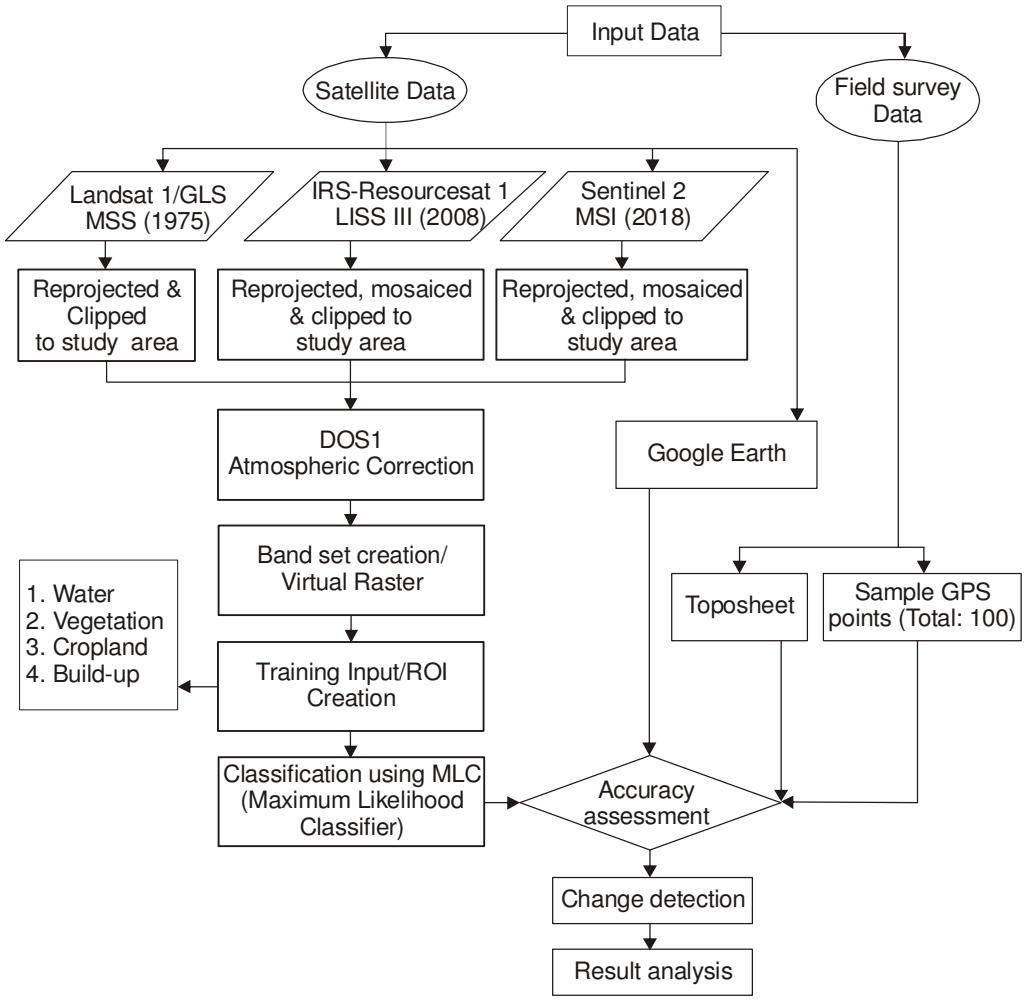

Fig. 4. Workflow of LULC in Shingla river basin.

III. RESULTS AND DISCUSSION

LULC maps of Shingla river basin generated in QGIS SCP using maximum likelihood classifier (MLC) are given in Fig. 6 for the years 1975, 2008 and 2018 respectively.

The challenges involved in data availability are overcome by the acquisition of satellite data and ground trothing using field survey data. Data from three different satellites viz. Landsat MSS (1975), Resource sat 1-LISS III (2008) and Sentinel 2-MSI (2008) are used along with ancillary data. Four land use and land cover classes are selected for the study. In terms of area, major land use and land cover classes in Shingla river basin during 1975-2008 are: vegetation > cropland > water bodies > built up (Table 2). Post 2008, rapid expansion in built up areas changed the LULC area order as: vegetation > cropland > built up> water bodies (Table 2). Results show that major decline in SRB LULC is in vegetation cover (Fig. 5) which decreased from 72.45% in 1975 to 62.38% in 2008 and further decreased to 58.91% by 2018. Built-up areas increased linearly from 3.71% in 1975 to 4.06% in 2008 and further increased to 12.24% by the end of 2018. However, temporal changes in croplands and water bodies are non-linear with croplands increasing from 17.46% (1975) to 22.49% (2008) and then decreased to 19.18% (2018). Similarly, water bodies increased from 6.37% (1975) to 11.06% (2008) and then decreased to 9.65% (2018).

Table 2: Area and percentage change in different land use and land cover categories of SRB during 1975 – 2018.

LULC Categories	1975		2008		2018		Change	
	Area (Km^2)	%	Area (Km^2)	%	Area (Km^2)	%	Area (Km^2)	%
Water	50.42	6.37	87.54	11.06	76.38	9.65	+25.96	3.28
Vegetation	573.49	72.45	493.78	62.38	466.31	58.91	-107.18	13.54
Cropland	138.2	17.46	178.02	22.49	151.82	19.18	+13.62	1.72
Built up	29.36	3.71	32.13	4.06	96.88	12.24	+67.52	8.53
Total	791		791		791			

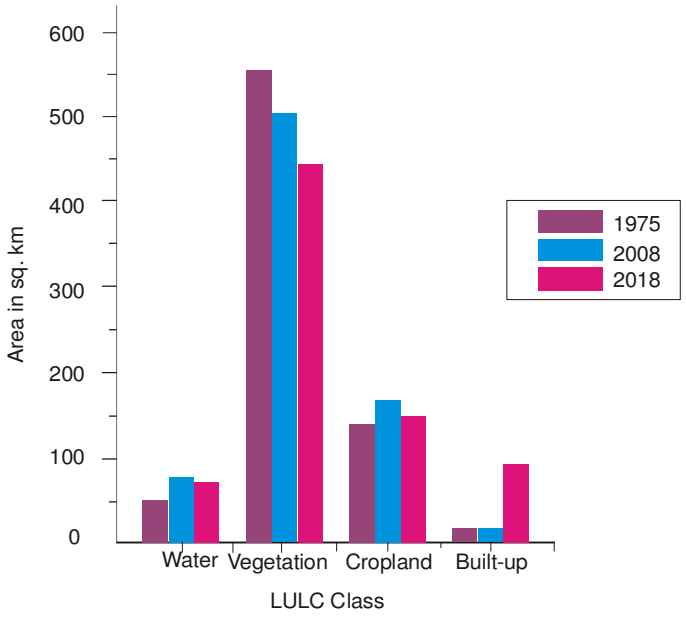

Fig. 5. Major Land Use and Land Cover classes in Shingla river basin in 1975, 2008 and 2018.

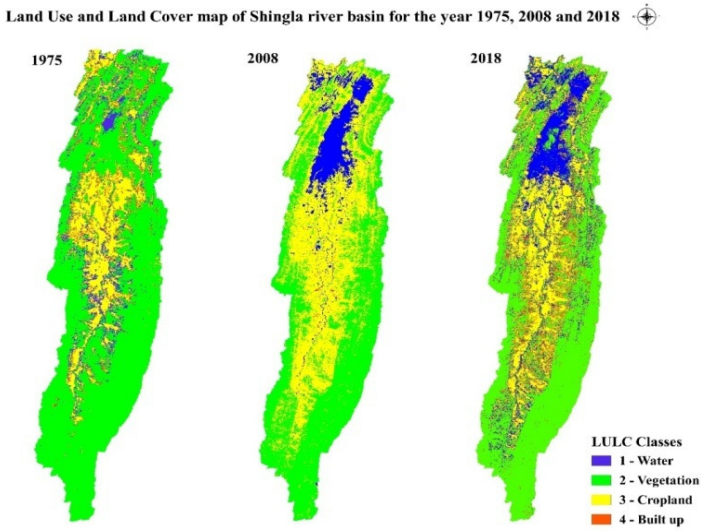

Fig. 6. Land Use and Land Cover change maps of Shingla river basin for the year 1975, 2008 and 2018.

A. Accuracy assessment

Quantification of map accuracies is done by creating an error matrix, also known as confusion matrix that compares the classification map with a reference map [23]. For ground truthing and accuracy assessment of the obtained results, ancillary and field survey data being essential, randomly 100 estimated GPS points are collected from the basin during field visits, based on the Eqn. (3) of [24] as stated below.

Random points are also collected from high resolution Google Earth imageries for the locations where access is difficult especially in the mountainous regions.

$$N = \{\sum_{i=1} \frac{(Wi-Si)}{So}\}^2 \quad (3)$$

where, Wi = mapped area proportion of class i

Si = standard deviation of stratum i

So = expected standard deviation of overall accuracy

Survey of India topo sheets (1:250 000 scale) were also used for accuracy assessment in case of Landsat 1 MSS (1975) satellite data. Kappa statistical analysis is used for accuracy assessment of the created LULC maps of Shingla river basin. Kappa analysis is a commonly used multi-variate statistical tool for accuracy assessment [25, 26].

The estimate of kappa method is known as K-HAT statistics and is calculated by the equation described by [27-29] as

$$\widehat{K} = \frac{N \sum_{i=1}^{r} X_{ij} - \sum_{i=1}^{r} X_i X_j}{N^2 - \sum_{i=1}^{r} X_i X_j} \quad (4)$$

where, r = Total number of rows and columns

N = Total number of observations

Xij = Total observation in row i and column j

Xi = Sum of values in row i

Xj = Sum of values in column j

Table 3: Results of kappa statistics.

Year	Producer's accuracy (%)				User's accuracy (%)				Overall accuracy (%)	Kappa/hat coefficient
	W	V	CL	BU	W	V	CL	BU		
1975	100.00	93.62	85.72	100.00	40.00	100.00	86.36	66.66	92.55	0.81
2008	100.00	94.23	93.11	100.00	70.00	98.33	92.00	60.00	92.60	0.86
2018	100.00	99.88	95.08	79.76	60.00	96.66	95.00	100.00	96.17	0.92

W= Water bodies, V= Vegetation, CL= Cropland, BU= Built-up areas.

Results of kappa statistical analysis are given in Table 3 with producer's, user's, overall accuracies and kappa hat statistics. Standard Kappa hat values range from 0 to 1. K value of 1 implies perfect agreement and K value less than 0 i.e. negative K value implies no agreement between the observed and the actual results. K values higher than 0.75 indicate an excellent agreement while lower than 0.4 indicates a poor agreement [25]. Overall LULC map accuracies are 92.55%, 92.60% and 96.17% with kappa hat values of 0.81, 0.86 and 0.92 for the respective years 1975, 2008 and 2018 (Table 3). Standard LULC maps require an optimum accuracy above 90% [30-31].

IV. CONCLUSION

Vegetation is the major land cover class in Shingla river basin which however reduced by 13.54% by 2018 (Table 2), indicating large scale deforestation over the last four decades as the cause for depletion. Agricultural cropland, the second major land use class increased by 1.72% by 2018. The trend in the change of cropland indicates conversion of forest cover to croplands between 1975 and 2008 but post 2008 the decline in croplands is due to increase in built up areas that increased from 3.75% to 12.24% in 2018 (Table 2). In the third major land use class, water bodies in the basin have increased by 3.28% (Table 2) over the last four decades and increase in water bodies is potentially due to increase in number of ponds, canals and flood plains. Son Beel wetland located in the downstream of Shingla river basin is the major water source. More croplands along the wetland have been converted into flood plains due to siltation and agricultural practice. This has though led to increase in water bodies, the actual wetland extent has decreased which is evident from the decrease in water from 11.06% to 9.65% in 2018.

V. FUTURE SCOPE

This being the first work of its kind on Shingla river basin, this study will be helpful for planners and decision makers in sustainable natural resource management and mitigation strategies.

ACKNOWLEDGEMENTS

The authors would like to thank UGC, Government of India for providing Scholarship (MANF) to First author. Authors would also like to thank Pondicherry Central University for providing the working facilities.

REFERENCES

[1]. Turner, M. G., & Gardner, R. H. (2015). Landscape Ecology in Theory and Practice. Springer-Verlag New York. doi:10.1007/978-1-4939-2794-4. 1-489.

[2]. Gibril, M. B. A., Bakar, S. A., Yao, K., Idrees, M. O., & Pradhan, B. (2017). Fusion of RADARSAT-2 and multispectral optical remote sensing data for LULC extraction in a tropical agricultural area. *Geocarto international*, *32*(7), 735-748.

[3]. Jiang, L., Li, C. Y., Song, B., & Li, S. S. (2015). Impacts of land use/cover changes on carbon storage in Beijing 1990–2010. *International Journal of Environmental Studies*, *72*(6), 972-982.

[4]. Desta, L., Kassie, M., Benin, S. and Pender, J. (2000). *Land degradation and strategies for sustainable development in the Ethiopian highlands: Amhara Region* (Vol. *32*). ILRI (aka ILCA and ILRAD). (Page No.)

[5]. Schultz, M., Voss, J., Auer, M., Carter, S., & Zipf, A. (2017). Open land cover from OpenStreetMap and remote sensing. *International journal of applied earth observation and geoinformation*, *63*, 206-213.

[6]. Wilk, J., & Hughes, D. A. (2002). Simulating the impacts of land-use and climate change on water resource availability for a large south Indian catchment. *Hydrological Sciences Journal*, *47*(1), 19-30.

[7]. Garg, V., Aggarwal, S. P., Gupta, P. K., Nikam, B. R., Thakur, P. K., Srivastav, S. K., & Kumar, A. S. (2017). Assessment of land use land cover change impact on hydrological regime of a basin. *Environmental Earth Sciences*, *76*(18), 1-17.

[8]. Munoth, P., & Goyal, R. (2019). Impacts of land use land cover change on runoff and sediment yield of Upper Tapi River Sub-Basin, India. *International Journal of River Basin Management*, 1-13.

[9]. Zhang, L., Karthikeyan, R., Bai, Z., & Srinivasan, R. (2017). Analysis of stream flow responses to climate variability and land use change in the Loess Plateau region of China. *Catena*, *154*, 1-11.

[10]. Neupane, R. P., & Kumar, S. (2015). Estimating the effects of potential climate and land use changes on hydrologic processes of a large agriculture dominated watershed. *Journal of Hydrology*, *529*, 418-429.

[11]. Butt, A., Shabbir, R., Ahmad, S. S., & Aziz, N. (2015). Land use change mapping and analysis using Remote Sensing and GIS: A case study of Simly watershed, Islamabad, Pakistan. *The Egyptian Journal of Remote Sensing and Space Science*, *18*(2), 251-259.

[12]. Dewan, A. M., & Yamaguchi, Y. (2009). Using remote sensing and GIS to detect and monitor land use and land cover change in Dhaka Metropolitan of Bangladesh during 1960-2005. *Environmental Monitoring and Assessment*, *150*(1-4), 237–249.

[13]. Sajjad, H., & Iqbal, M. (2012). Impact of urbanization on land use/land cover of Dudhganga watershed of Kashmir Valley, India. *International Journal of Urban Sciences*, *16*(3), 321-339.

[14]. Chakravarty, H. & Singha, H. (2015). Avian Diversity in and around Son Beel, Assam. *Asian Journal of Advanced Basic Sciences*, *3*(2), 147–153.
[15]. Khan, A. S., Khan, A. B., & Khan, H. H. (2016). Flood Inundation Mapping of Shingla River Basin in Assam Using a Distributed Hydrological Model. *The Ecoscan, 10*(3-4), 405–409.
[16]. Ruelland, D., Tribotte, A., Puech, C., & Dieulin, C. (2011). Comparison of methods for LUCC monitoring over 50 years from aerial photographs and satellite images in a Sahelian catchment. *International Journal of Remote Sensing*, *32(*6), 1747–1777.
[17]. Massod, H., Sheeba, A., Zamir, U. B., & Kazmi, J. H. (2015). Application of Comparative Remote Sensing Techniques for Monitoring Mangroves in Indus Delta, Sindh, Pakistan. *Biological Forum-An International Journal*, *7*(1), 783–792.
[18]. QGIS Development Team, (2019). QGIS Version 3.8.2. QGIS Project. Open Source Geospatial Foundation Project. Retrieved from http://qgis.osgeo.org.
[19]. Colney, L., & Nautiyal, B. P. (2013). Characterization and evaluation of soils of Aizwal district, Mizoram, India using remote sensing and GIS technology. *Journal of Geomatics*, *7*(1), 83–91.
[20]. Pinto, L. C., de Mello, C. R., Owens, P. R., Norton, L. D., & Curi, N. (2016). Role of inceptisols in the hydrology of mountainous catchments in southeastern Brazil. *Journal of Hydrologic Engineering*, *21*(2), 1–10.
[21]. Vadivelu, S., Sen, T. K., Bhaskar, B. P., Baruah, U., Sarkar, D., Maji, A. K., & Gajbhiye, K. S. (2004). Soil Series of Assam. (NBSS, Publ.*101*: 1-229.
[22]. Choudhury, P., & Islam, M. (2016). Status survey of Western Hoolock Gibbon and conservation initiative through Mass awareness in the Reserve Forest areas of Barak valley, Assam, India. UGC Major Research project, New Delhi, India, 1-107.
[23]. Rouse, J. W., Haas, R. H., Schell, J. A., & Deering, D. W. (1974). Monitoring vegetation system in the great plains with ERTS. Proceedings of the Third Earth Resources Technology Satellite-1 Symposium, USA; NASA, Paper A *20*: 3010–3017.
[24]. FAO. (2016). Map accuracy assessment and area estimation : a practical guide. National forest monitoring assessment working paper, 46 E, 1-69.
[25]. Olofsson, P., Foody, G. M., Herold, M., Stehman, S. V., Woodcock, C. E., & Wulder, M. A. (2014). Good practices for estimating area and assessing accuracy of land change. *Remote Sensing of Environment*, *148*, 42–57.
[26]. Cohen, J. (1960). A coefficient of agreement for nominal scales. *Educational Psychology Measurement*, *20*(14), 37–46.
[27]. Smits, P. C., Dellepiane, S. G., & Schowengerdt, R. A. (1999). Quality assessment of image classification algorithms for land-cover mapping: A review and a proposal for a cost-based approach. *International Journal of Remote Sensing*, *20*(8), 1461–1486.
[28]. Bishop, Y. M., Fienberg, S. E., & Holland, P. W. (1975). Discrete Multivariate Analysis: Theory and Prictice. MIT Press, Cambridge, MA, 1-30.
[29]. Congalton, R. G., & Mead, R. A. (1983). A quantitative method to test for consistency and correctness of photointerpretation. *Photogrammetric Engineering and Remote Sensing, 49*(1), 69–74.
[30]. Banko, G. (1998). A Review of Assessing the Accuracy of Classifications of Remotely Sensed Data and of Methods Including Remote Sensing Data in Forest Inventory. *Interim Report of International Institute for Applied Systems Analysis*, *A-2361*, Laxenburg, Austria 1–36.
[31]. Lea, C., & Curtis, A. C. Natural Resource, (2010). Thematic accuracy assessment procedures: National Park Service Vegetation Inventory version 2.0. Natural Resource Report NPS/2010/NRR–2010/204, Fort Collins, Colorado, USA, 1-90.

How to cite this article: Khan, S.A. and Khan, Anisa Basheer (2020). Assessment of Land Use and Land Cover Dynamics in Shingla River Basin Using Multi Temporal Satellite Imageries. *International Journal on Emerging Technologies*, *11*(1): 263–269.